processes

MDPI

Article

The Microstructure and Mechanical Properties of a Dissimilar Rotary Friction Welded TC4 Titanium Alloy to 304SS Stainless Steel with Inconel 718 Alloy Interlayer

Rui Tang [1,2,*] and Chunquan Li [1,*]

[1] Guilin University of Electronic Technology, No. 1 Jinji Road, Qixing District, Guilin 541004, China
[2] Guangzhou Huadu District Productivity Promotion Center, No. 67 Tiangui Road, Huadu District, Guangzhou 510800, China
* Correspondence: tangrui791021@163.com (R.T.); lcq@guet.edu.cn (C.L.)

Abstract

This study investigates the microstructure and mechanical properties of a dissimilar joint formed by rotary friction welding, which joins TC4 titanium alloy to 304 stainless steel using an Inconel 718 interlayer. The welding parameters were as follows: a friction time of 9 s, a friction pressure of 160 MPa, an upset time of 2 s, a forging pressure of 250 MPa, and a rotational speed of 1400 rpm. Microstructural analysis revealed the formation of intermetallic compounds (IMCs), including Fe_2Ti, Ni_3Ti, NiCrFe, $FeNi_3$, Ti_2Ni, and FeNi, at the TC4/Inconel 718 interface, while Ni_3Ti and $FeNi_3$ IMCs were identified at the Inconel 718/304SS interface. The tensile tests demonstrated that the joint with the Inconel 718 interlayer (TC4/Inconel 718/304SS) achieved an ultimate tensile strength (UTS) of 717.73 MPa and an elongation of 13.05%. In contrast, the direct joint without the interlayer (TC4/304SS) exhibited a lower UTS of 631.58 MPa and a reduced elongation of 7.39%. Therefore, the introduction of the Inconel 718 interlayer significantly improved joint quality, increasing tensile strength by 13.64% and elongation by 76.59%. More importantly, the interlayer effectively inhibited the formation of brittle Ti-Fe intermetallic compounds, which are typically detrimental to joint performance.

Keywords: rotary friction welding; TC4 titanium alloy/304SS stainless steel; dissimilar joining; mechanical property; microstructure; Inconel 718 alloy interlayer

1. Introduction

Rotary friction welding (RFW) is a solid-state welding process in which two workpieces are joined under pressure. Frictional heat is generated at temperatures below the melting points of the base materials [1]. This process offers numerous advantages, including the absence of smoke and harmful gases, no pollution, a joint formed in the solid state without melting, high precision, suitability for high-speed operation, and cost-effectiveness [2]. Driven by advancements in manufacturing and increasingly diverse industrial demands, rotary friction welding of dissimilar metals has attracted significant attention [3].

Titanium alloys are characterized by high specific strength, excellent corrosion resistance, and good toughness across a wide temperature range. However, their high cost limits their wider application. Combining titanium alloys with steel can leverage the complementary advantages of both materials, making such composite structures highly valuable in aerospace, chemical, medical, and marine engineering [4–6]. Nonetheless, significant challenges arise due to the considerable differences in thermomechanical properties and the

Check for updates

Academic Editor: Qingmin Yu

Received: 4 December 2025
Revised: 28 December 2025
Accepted: 4 January 2026
Published: 6 January 2026

Copyright: © 2026 by the authors. Licensee MDPI, Basel, Switzerland. This article is an open access article distributed under the terms and conditions of the Creative Commons Attribution (CC BY) license.

limited mutual solubility between Ti and Fe. These factors readily promote the formation of brittle Ti-Fe intermetallic compounds (IMCs) at the joint interface, which can severely degrade the connection strength [7–9].

Rotary friction welding (RFW) of titanium to steel operates at relatively lower temperatures and shorter cycle times compared to many fusion welding processes. This characteristic helps to suppress detrimental metallurgical reactions and minimize residual stresses. In the literature, studies on the weldability of steel and titanium by rotary friction welding focus on optimizing process parameters by analyzing the microstructure and tensile strength of the joints [5,10–18].

The dissimilar welding of titanium and steel combines the superior properties of both materials. A key challenge is controlling the formation of brittle Ti-Fe intermetallic compounds (IMCs) at the interface. To address this, interlayers—including copper [19,20], silver [21,22], nickel [23–29], and aluminum alloys [30]—have been introduced. Notably, multi-component alloys, particularly nickel-based alloys, are effective in suppressing harmful IMCs and enhancing joint strength and ductility [31,32]. Despite these strategies, many joints still suffer from low strength and brittle fractures, underscoring the inherent difficulty in completely eliminating brittleness. Consequently, further in-depth investigation into rotary friction welding for such dissimilar combinations is not only necessary but critically important.

This study aims to investigate the influence of an Inconel 718 alloy interlayer on the microstructure and mechanical properties of dissimilar rotary friction-welded joints between TC4 and 304SS. The primary function of the interlayer is to inhibit the interdiffusion of Fe and Ti elements, thereby reducing the formation of brittle Fe-Ti and Fe-Cr-Ti intermetallic compounds (IMCs) and ultimately improving joint performance. As a continuation of prior research, this work seeks to provide deeper insights into how the rotary friction welding process affects the microstructure and mechanical properties of TC4/Inconel 718/304SS dissimilar joints. The melting behavior and interface reaction mechanisms of the Inconel 718 interlayer during rotational friction welding TC4/Inconel 718/304SS. The synergistic diffusion laws of multiple elements (Ni, Cr, Fe, Mo, Nb, Al, Ti) across the TC4/Inconel 718 and Inconel 718/304SS interfaces. The influence of RFW process parameters on the precipitation behavior of strengthening phases within the Inconel 718 interlayer itself. The underlying mechanism by which the Inconel 718 interlayer regulates the mechanical properties of the resultant joint. An assessment of the cost-effectiveness and engineering applicability of using an Inconel 718 interlayer for dissimilar metal RFW. This investigation will provide a novel technical pathway and theoretical foundation for achieving high-quality, cost-effective joining of TC4/304SS dissimilar metals.

2. Materials and Methods

2.1. Materials

In this study, dissimilar rotary friction welding was performed between TC4 and 304SS using an Inconel 718 alloy interlayer. All materials were in the form of cylindrical rods with a diameter of 20 mm. The lengths of the TC4 and 304SS rods were 75 mm, while the Inconel 718 interlayer rod was 23 mm long. The dimensions of the assembled specimens are illustrated in Figure 1. The specimen's welded distances were measured equally at 6 mm between the end and the middle stage. The faying surfaces for rotary friction welding were prepared by turning, and the surface roughness was 1.0 μm (Ra = 1.0 μm). The chemical compositions of the base metals (TC4 and 304SS) and the Inconel 718 interlayer are provided in Table 1.

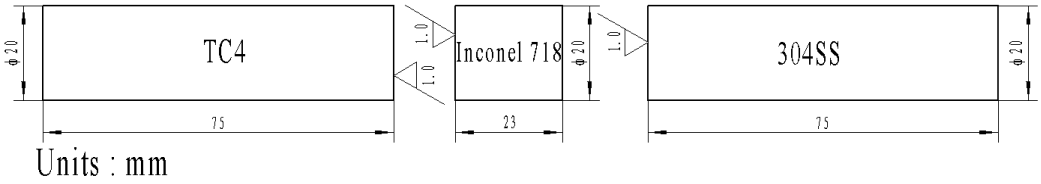


Figure 1. Processing diagram of the dissimilar rotary friction-welded TC4 to 304SS with Inconel 718 alloy interlayer.

Table 1. Chemical composition of the TC4/304SS base metals and Inconel 718 alloy.

Base Metal	Composition (wt.%)							
TC4	Al	V	Si	Fe	Cr	Mo	Mn	Ti
	5.60	3.29	0.20	0.18	-	-	-	90.73
304SS	C	Mn	Si	Ni	Cr	Al	V	Fe
	0.07	1.31	0.44	8.03	18.52	-	-	71.63
Inconel 718	Al	Ti	Cr	Fe	Nb	Mo	Ni	
	0.47	0.86	17.9	17.20	4.75	3.04	55.78	

2.2. The Rotary Friction Welding Process

The dissimilar joint of TC4 titanium alloy, Inconel 718 alloy, and 304 stainless steel (designated as TC4/Inconel 718/304SS) was fabricated using a rotary friction welding machine (Model: C-25A-2, Manufacturer: Changchun Welding Machine Factory, Changchun, China). A schematic diagram of the experimental setup is shown in Figure 2.

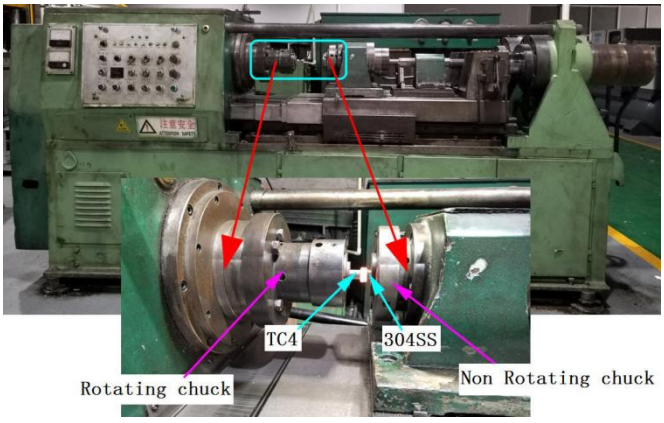


Figure 2. Experimental setup for the TC4/Inconel 718 alloy/304SS welded joints.

Before welding, the base metal rods were face-turned and ultrasonically cleaned in alcohol and acetone to remove surface oxides and contaminants. The welding parameters are listed in Table 2. The welding process consisted of two stages. In the first stage, the TC4 rod was clamped in the stationary vice, while the Inconel 718 rod was held in the rotating chuck, as shown in Figure 3a. Rotary friction welding was then performed to produce the TC4/Inconel 718 dissimilar joint. Before the second welding stage, the excess material on the Inconel 718 side of the TC4/Inconel 718 joint was machined off, leaving a precise 1 mm thickness of Inconel 718, as illustrated in Figure 3b. This prepared sub-assembly (TC4/Inconel 718 with a 1 mm layer) was then clamped in the rotating chuck. Subsequently, the 304SS rod was fixed in the stationary vice. Finally, the second rotary friction welding cycle was conducted to join this sub-assembly to the 304SS rod, thereby fabricating the complete TC4/Inconel 718/304SS tri-material joint.

Table 2. Friction welding parameters.

Friction Pressure (MPa)	Friction Time (s)	Welding Speed (rpm)	Upset Pressure (MPa)	Upset Time (s)
160	9	1400	250	2



Figure 3. (**a**) A picture of the TC4/Inconel 718 alloy welded joints, and (**b**) a picture of the TC4/Inconel 718 alloy/304SS welded joints.

2.3. Mechanical Property Tests

After rotary friction welding, the flash was removed by machining to eliminate potential micro-cracks that could initiate fracture under low loads. Tensile specimens were then extracted from the two dissimilar welded joints. The specimen dimensions are shown in Figure 4, and their machining adhered to the standard for bar-type tensile specimens.

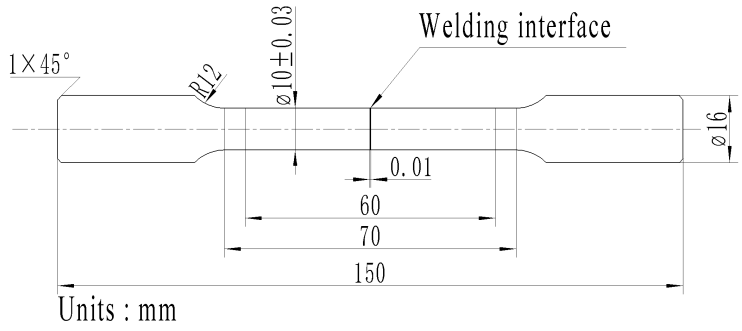


Figure 4. Tensile specimen size of the TC4, 304SS, and TC4/Inconel 718 alloy/304SS welded joints.

Tensile testing was performed at room temperature using a universal testing machine (Make: ZWICK, Ulm, Germany; Model: Z100), in accordance with the Chinese national standards GB/T 2649-89 ("Sampling Method for Mechanical Property Tests of Welded Joints") and GB/T 2651-2008 ("Tensile Test Method on Welded Joints").

For each joint configuration, three specimens were tested. The reported tensile strength represents the average value of these three tests.

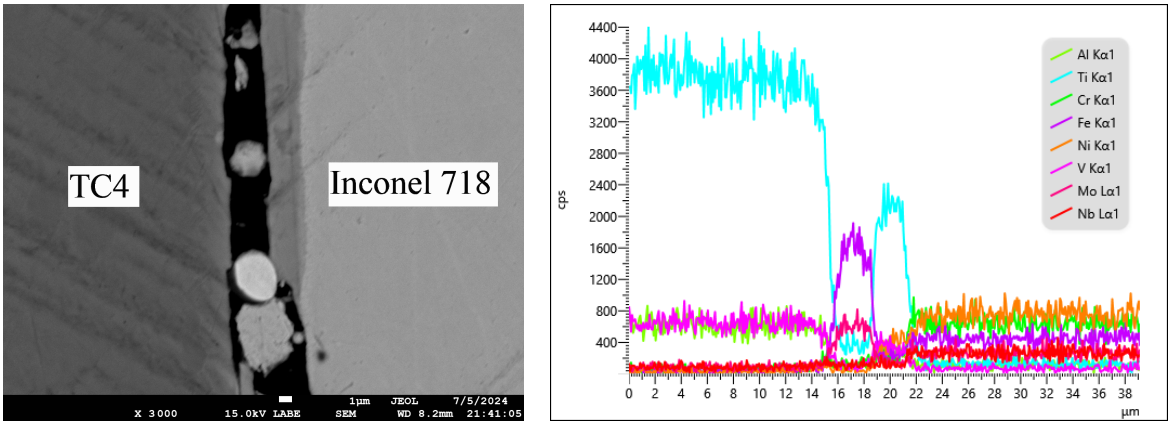
3. Results and Discussion

3.1. Microstructure

To further observe the morphology of the welded seam, a scanning electron microscope was used to observe the welded seam area. The microscopic characteristics of the welded interface were studied by field emission scanning electron microscopy (SEM, JSM-6360LV, JEOL Ltd., Tokyo, Japan) with energy dispersive spectroscopy (EDS), and the X-ray

diffraction (XRD, a Cu Kα radiation source, 1820, Philips, Amsterdam, The Netherlands) with an X-ray source in the 2θ range of 5–80°. A scanning electron microscope (SEM) was used to observe the microstructure of the joint. Energy dispersive spectroscopy (EDS) was used to analyze the composition of the interface micro zone and determine the concentration changes of elements in specific directions, Determine the phase composition of interface compounds using the X-ray diffraction (XRD).

Figure 5b presents the surface elemental distribution at the TC4/Inconel 718 welded interface, revealing a distinct diffusion zone primarily composed of Al, Ti, Cr, Fe, Ni, V, Mo, and Nb.



(**a**) (**b**)

Figure 5. SEM images of the center of the welded interface of the TC4/Inconel 718 alloy side of the TC4/Inconel 718 alloy/304SS welded joint.

The elemental interdiffusion is quantitatively detailed in the EDS line scan profile across the interface (Figure 5a). From the TC4 side towards the Inconel 718 side: the concentrations of Ti, Al, and V decrease continuously. Notably, Ti exhibits a complex profile: it decreases from the TC4 base metal, reaches a minimum at the interface, shows a slight increase, and then decreases again within the Inconel 718. The concentrations of Ni, Cr, and Nb increase progressively. The Fe and Mo profiles peak at the interface before decreasing on both sides.

This interdiffusion, particularly of Ti, Ni, Fe, Al, Cr, Mo, and V, is facilitated by their mutual solubility, which likely contributes to enhanced metallurgical bonding between TC4 and Inconel 718 [33]. The corresponding diffusion distances for key elements are illustrated in Figure 6a–d.

Figure 7b displays the surface elemental distribution across the Inconel 718/304SS welded interface, indicating the formation of a diffusion zone predominantly consisting of Fe, Cr, Ni, and Nb.

Quantitative EDS line-scan analysis across this interface (Figure 7a) reveals the following diffusion trends from the Inconel 718 side towards the 304SS side: The concentrations of Ni and Nb exhibit a continuous decreasing trend, with both elements diffusing into the 304SS side. The Fe concentration shows a corresponding increase, with significant diffusion of Fe into the Inconel 718 side. The Cr concentration remains relatively stable across the interface and in both base metals. This interdiffusion of Fe, Cr, Ni, and Nb, driven by their mutual solubility, is likely a key factor in promoting metallurgical bonding between Inconel 718 and 304SS. The measured diffusion distances for these elements are further quantified in Figure 8a–d.

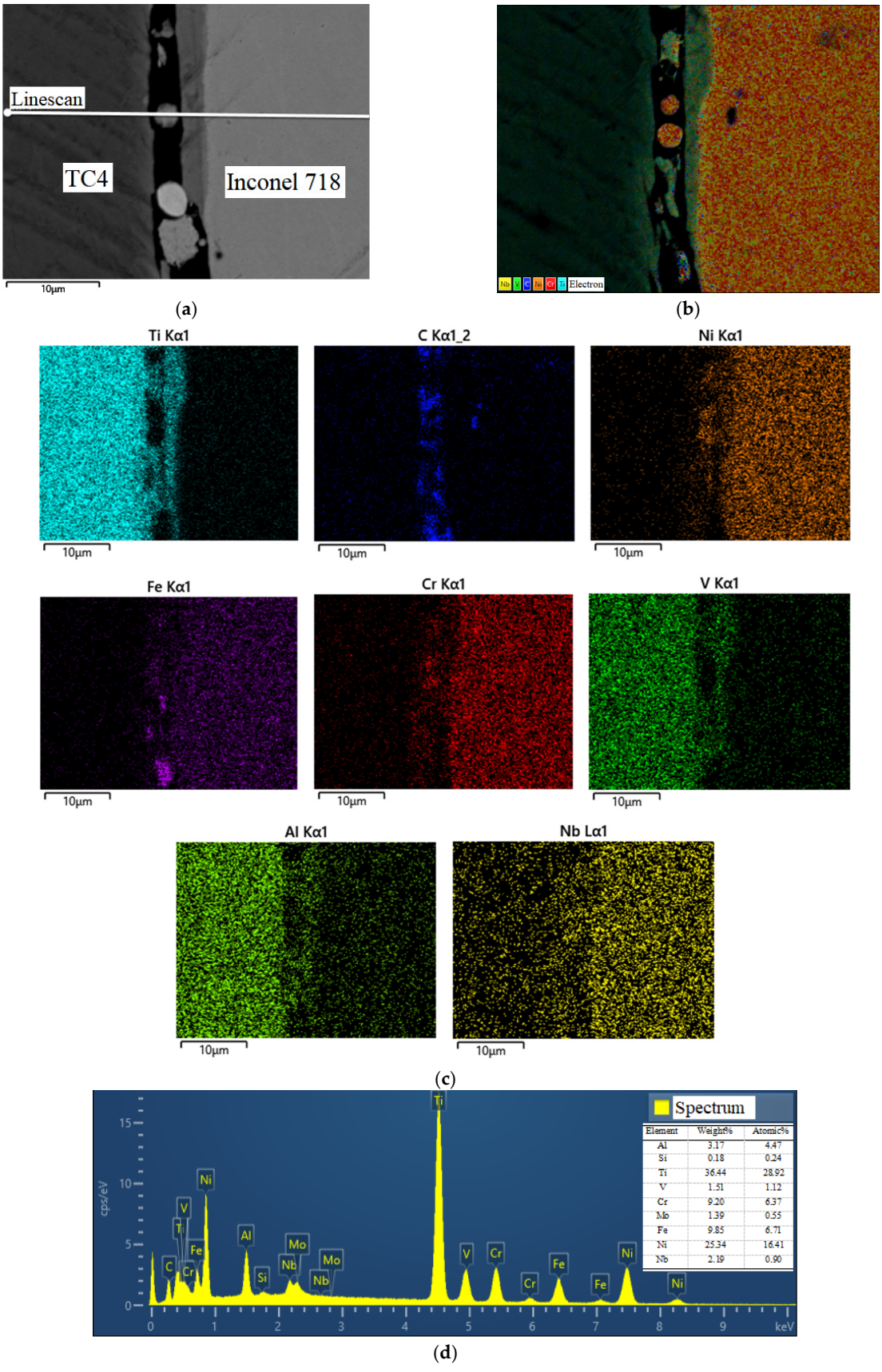
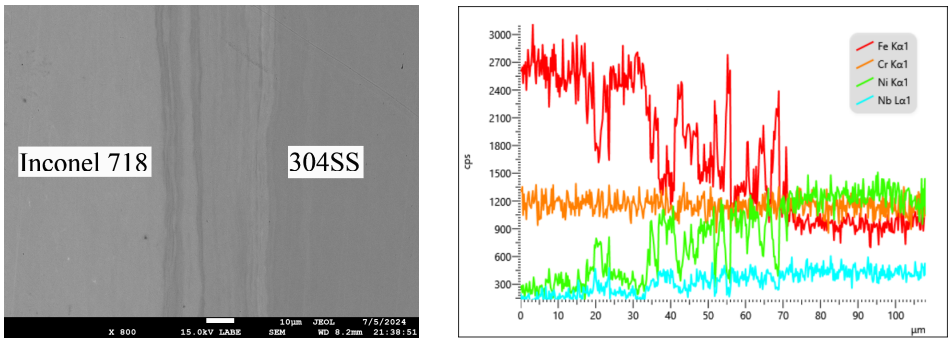
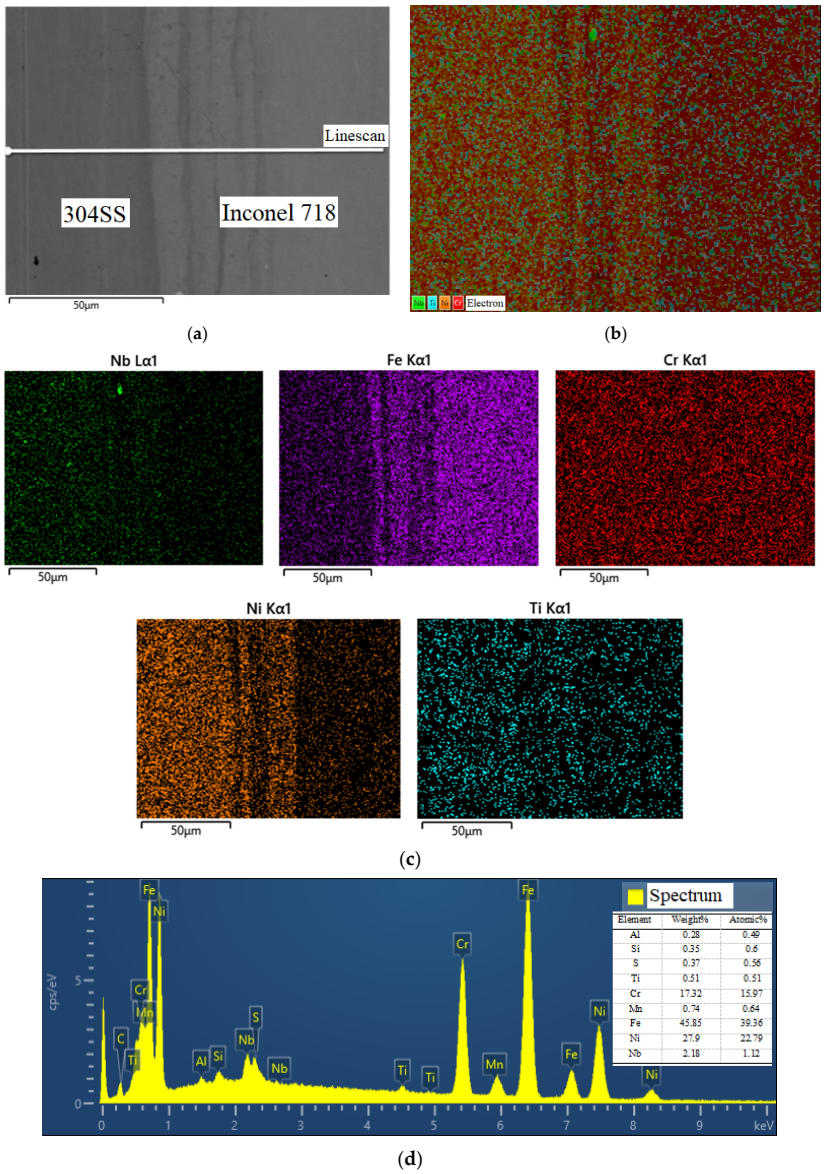


Figure 6. Rotary friction welded joint: (**a**) SEM microstructure, (**b**) surface distribution of elements at the TC4/Inconel 718 alloy welded interface, (**c**) elemental mapping of the TC4/Inconel 718 alloy side of the TC4/Inconel 718/304SS welded joint, and (**d**) show EDS spectra obtained from the TC4/Inconel 718 welded interface with line scan.



(**a**) (**b**)

Figure 7. SEM (scanning electron microscope) images of the center of the 304SS/Inconel 718 side of the TC4/Inconel 718 alloy/304SS welded joint.



(**c**) (**d**)

Figure 8. Rotary friction-welded joint: (**a**) SEM microstructure, (**b**) surface distribution of elements at the Inconel 718/304SS welded interface, (**c**) elemental mapping of the Inconel 718/304SS side of the TC4/Inconel 718/304SS welded joint, and (**d**) shows EDS spectra obtained from the 304SS/Inconel 718 welded interface with line scan.

3.2. XRD Analysis on the Welded Surfaces

The fracture surfaces of the tensile-tested samples were examined by XRD. Figure 9 presents the XRD patterns obtained from both sides of the dissimilar rotary friction-welded TC4/304SS joint. The pattern from the TC4 side revealed the presence of Ti, $Ti_{1.83}Zr_{0.17}$, $NiTi_{0.92}$, and $Fe_{0.2}Ti_{0.8}$ phases. In contrast, the pattern from the 304SS side primarily contained phases such as Fe, $Cr_{0.7}Fe_{0.3}$, δ-Fe, and γ-Fe.

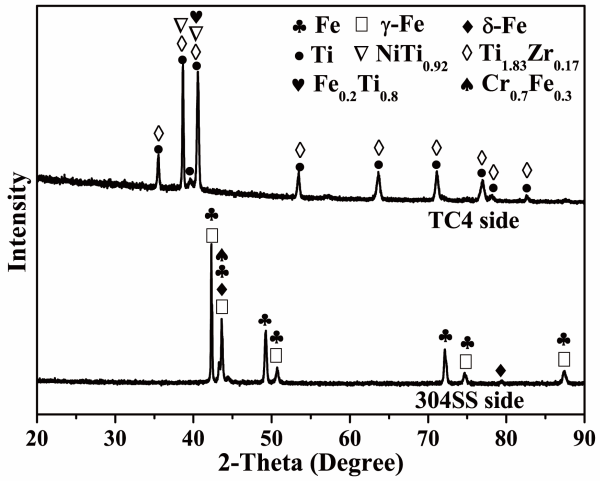


Figure 9. XRD (X-ray diffraction) results of the dissimilar rotary friction-welded TC4/304SS joints.

The phase composition across the dissimilar TC4/Inconel 718/304SS joint was characterized by XRD, as shown in Figure 10. The analysis revealed distinct phase constituents on each side of the joint: On the TC4 side, the primary phases identified were Ti, Fe_2Ti, Ni_3Ti, NiCrFe, $FeNi_3$, Ti_2Ni, Ni, and FeNi. On the 304SS side, the detected phases included Ni_3Ti, $FeNi_3$, and γ-Fe. On the Inconel 718 interlayer side, the main phases were NiCrFe, $FeNi_3$, Ti_2Ni, FeNi, and Ni.

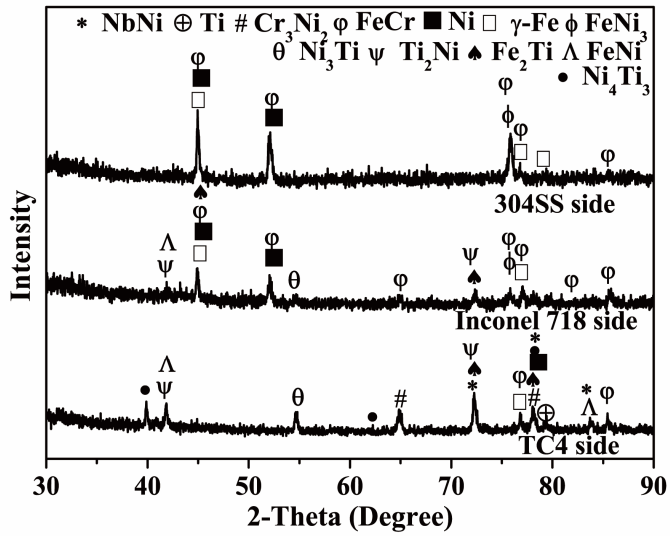


Figure 10. XRD (X-ray diffraction) results of the dissimilar rotary friction-welded TC4/304SS joints with Inconel 718 alloy interlayer.

XRD analysis confirmed the formation of brittle intermetallic compounds (IMCs), such as $Fe_{0.2}Ti_{0.8}$ and $Cr_{0.7}Fe_{0.3}$, at the interface of the direct TC4/304SS joint. In contrast, the joints fabricated with the Inconel 718 alloy interlayer exhibited a different phase composition. At the TC4/Inconel 718 alloy interface, IMCs like Fe_2Ti and NiCrFe were identified,

while at the Inconel 718/304SS interface, the detrimental Fe-Ti and Fe-Cr-Ti IMCs were effectively suppressed.

These results demonstrate that the Inconel 718 alloy interlayer acts as an effective diffusion barrier. It inhibits the direct interdiffusion of Fe and Ti, thereby significantly reducing the formation of brittle Fe-Ti and Fe-Cr-Ti compounds, which is the primary mechanism for the enhanced joint strength.

3.3. Mechanical Properties

3.3.1. Microhardness

The Vickers microhardness measurements were used to evaluate the hardness distribution of rotary friction-welded joints. The hardness tests were performed according to GB/T 4340.1-2024 "Standard test method for Vickers Hardness of Metallic Materials" using a Vickers microhardness instrument (Foshan Broway Measuring Instrument Co., LTD., Digital Vickers Hardness tester, BRV-610B, China). The microhardness measurements were carried out from the 304SS side to the TC4 side at the center of the welded rod with a load of 100 N, dwell time of 15 s, and center-to-center spacing of 1 mm.

Figure 11 shows the Vickers microhardness profile across the TC4/304SS rotary friction-welded joint with the Inconel 718 alloy interlayer. The measurements were carried out from the 304SS side to the TC4 side. The formula for calculating the Vickers hardness value is provided based on the literature [34,35].

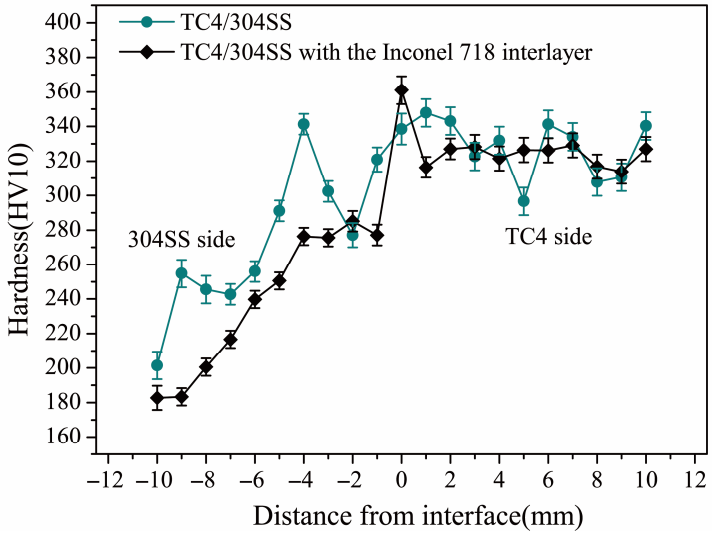


Figure 11. Distribution of Vickers microhardness across the dissimilar rotary friction-welded TC4/304SS and TC4/Inconel 718/304SS joints.

The microstructure and hardness of the TC4/Inconel 718 alloy/304SS welded seam and the heat-affected zone show significant differences from the base metals, often resulting in stress concentration occurring in the welded seam or the heat-affected zone rather than the base metals [36].

The Vickers hardness value on the 304SS side gradually increases, and near the welded seam reached a maximum of 285.1 ± 10 HV10. The Vickers hardness value on the Inconel 718 alloy interlayer side, close to the welded interface, reached maximum values of 361.0 ± 10 HV10. The Vickers hardness value on the TC4 side is slightly larger than that of the TC4 base metal, and near the welded seam reached a maximum of 328.2 ± 10 HV10 and decreased rapidly from the welded seam until the base metal.

The Vickers hardness of the TC4/304SS welded joint without an interlayer fluctuates greatly on the 304SS side, reaching the maximum value 341.3 ± 10 HV10 near the welded

seam, while the Vickers hardness of the TC4 side fluctuates slightly, reaching the maximum value 347.9 ± 10 HV10 near the welded seam. The Vickers hardness value 338.5 ± 10 HV10 of the TC4/304SS welded joint without an interlayer at the welded seam was lower than the Vickers hardness value 361 ± 10 HV10 of the TC4/304SS welded joint with Inconel 718 interlayer at the welded seam.

3.3.2. Tensile Strengths

Tensile specimens of the TC4/304SS base metals and dissimilar TC4/304SS and dissimilar rotary friction-welded TC4/304SS with Inconel 718 alloy interlayer after testing are depicted in Figure 12. The typical engineering stress-strain curves of the TC4/304SS base metals and the dissimilar rotary friction welded TC4/304SS, and the dissimilar rotary friction welded TC4/304SS with the Inconel 718 alloy interlayer are displayed in Figure 13.

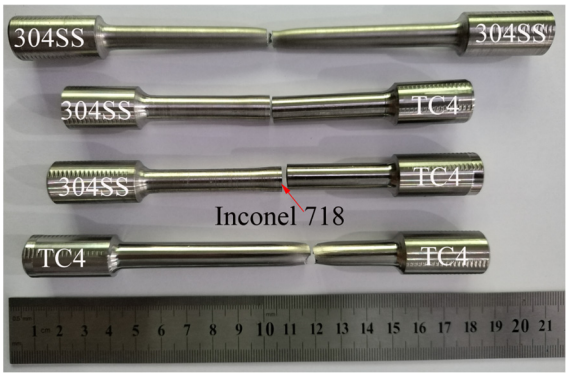


Figure 12. Bar tensile specimens of the TC4/304SS base metals and the dissimilar rotary friction-welded TC4/304SS and TC4/304SS with the Inconel 718 interlayer.

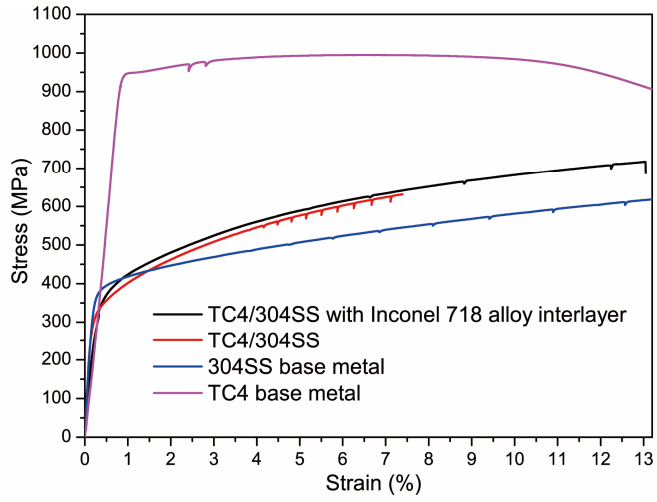


Figure 13. Typical engineering stress-strain curves of the TC4/304SS base metals and the dissimilar rotary friction welded TC4/304SS, and the dissimilar rotary friction welded TC4/304SS with the Inconel 718 alloy interlayer.

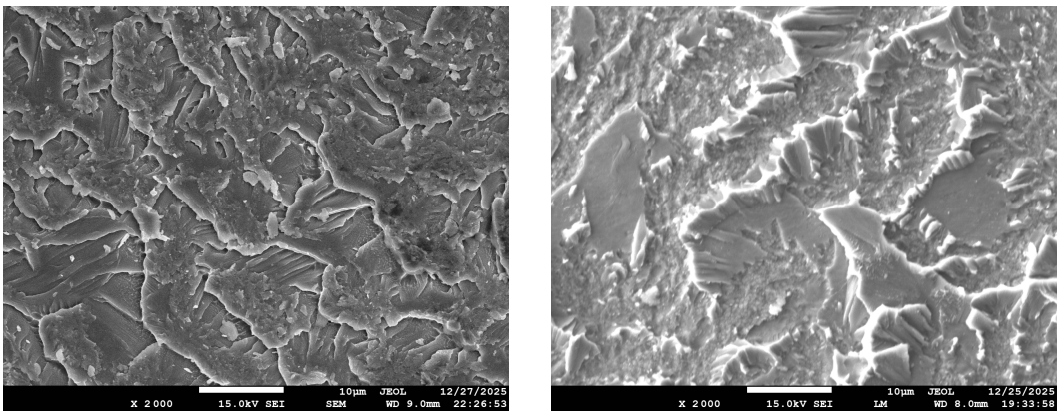
The tensile properties of the joint were studied. The yield strength of the dissimilar rotary friction-welded TC4/304SS joints with the Inconel 718 alloy interlayer reached 354.77 MPa, and the ultimate tensile strength of the welded joints reached 717.73 MPa, and the maximum elongation of the welded joints reached 13.05%. The yield strength of the dissimilar rotary friction-welded TC4/304SS joints reached 336.14 MPa, and the ultimate tensile strength of the welded joints reached 631.58 MPa, and the maximum elongation of the joints reached 7.39%.

The yield strength, the ultimate tensile strength, and the elongation values were presented in Table 3. The failure of the tensile specimens of the dissimilar rotary friction-welded TC4/304SS and TC4/304SS with Inconel 718 alloy interlayer is shown in Figure 12. All of the welded specimens were found to fail in the welded interface. The welded specimens of TC4/304SS joints and TC4/304SS joints with Inconel 718 alloy interlayer showed lower tensile strengths compared with the TC4 and the 304SS base metals. The welded specimens of the TC4/304SS joints and the TC4/304SS joints with Inconel 718 alloy interlayer showed lower yield strengths compared with the TC4 and the 304SS base metals.

Table 3. Results of room temperature tensile testing (average properties from three tests in each case).

Sample	Yield Strength (MPa)	Tensile Strength (MPa)	Elongation (%)
TC4 base metal	949.00 ± 9	994.90 ± 5	15.53 ± 0.8
304SS base metal	380.57 ± 7	746.15 ± 9	52.98 ± 0.9
TC4/304SS	336.14 ± 3	631.58 ± 8	7.39 ± 0.5
TC4/Inconel 718/304SS	354.77 ± 5	717.73 ± 8	13.05 ± 0.7

From the macroscopic fracture morphology and microscopic morphology, it can be seen that the fracture mechanism is mainly brittle fracture. As shown in Figure 14. There is plastic deformation in the welded area. The results of the tensile test confirm the conclusions of other researchers [37–41].



(**a**) (**b**)

Figure 14. Fractography of the dissimilar rotary friction-welded TC4/Inconel 718 alloy/304SS joint. (**a**) TC4 side and (**b**) 304SS side.

It can be seen that in order to achieve better connection quality, adding intermediate connectors can improve the softening effect, accelerate the connection, eliminate the phenomenon of virtual connection, and effectively improve the mechanical properties of TC4/304SS connection [9]. The content of the brittle intermetallic compounds Fe-Ti and Fe-Cr-Ti was reduced, and the performance of the joints was improved. The addition of the Inconel 718 alloy interlayer made the welded joint more solid, and enhanced the welded strength by 13.64%, and enhanced the welded elongation by 76.59%.

4. Conclusions

This work investigated the effect of an Inconel 718 alloy interlayer on the microstructure and mechanical properties of rotary friction-welded dissimilar joints between TC4 titanium alloy and 304 stainless steel. Based on the experimental results, the following conclusions can be drawn:

1. The tensile properties of the joints with and without the Inconel 718 interlayer are compared as follows: For the TC4/Inconel 718/304SS joint: yield strength = 354.77 MPa, ultimate tensile strength (UTS) = 717.73 MPa, elongation = 13.05%. For the direct TC4/304SS joint: yield strength = 336.14 MPa, UTS = 631.58 MPa, elongation = 7.39%. The introduction of the Inconel 718 interlayer significantly enhanced the joint performance, increasing the UTS by 13.64% and the elongation by 76.59% compared to the direct joint.

2. XRD analysis of the fracture surfaces revealed distinctly different phase constituents between the two joint types, which correlate with their mechanical performance. For the direct TC4/304SS joint, brittle Ti-Fe and Cr-Fe intermetallic compounds (IMCs), such as $Ti_{1.83}Zr_{0.17}$, $NiTi_{0.92}$, $Fe_{0.2}Ti_{0.8}$, and $Cr_{0.7}Fe_{0.3}$, were predominant. For the TC4/Inconel 718/304SS joint, the phase composition was more complex and distributed across the interfaces. The TC4 side contained IMCs like Fe_2Ti, Ni_3Ti, NiCrFe, $FeNi_3$, Ti_2Ni, and FeNi. The 304SS side contained Ni_3Ti and $FeNi_3$, while the Inconel 718 alloy side featured NiCrFe, $FeNi_3$, Ti_2Ni, and FeNi. The presence of brittle Fe-Ti/Cr-Fe IMCs in the direct joint explains its inferior strength and ductility. In contrast, the Inconel 718 alloy altered the reaction products, suppressing the most detrimental brittle phases and contributing to the joint's enhanced properties.

3. The Vickers hardness exhibited significant variations in the vicinity of the weld across the three materials. On the 304SS side, the hardness increased progressively towards the weld interface, reaching a peak value of 285.1 $\pm$ 10 HV10. The maximum hardness values for the Inconel 718 alloy and the TC4 side were 361.0 $\pm$ 10 HV10 and 328.2 $\pm$ 10 HV10, respectively. The peak hardness on the TC4 side was slightly higher than that of its base metal. Notably, the hardness on the TC4 side decreased sharply from the weld seam towards the base metal.

4. The analysis of the TC4/Inconel 718/304SS welded joints revealed that intermetallic compounds such as Fe_2Ti, Ni_3Ti, NiCrFe, $FeNi_3$, Ti_2Ni and FeNi formed at the TC4/Inconel 718 interface, and Ni_3Ti and $FeNi_3$ at the Inconel 718/304SS interface. However, the formation of brittle titanium-steel IMCs was effectively suppressed throughout the joint.

Author Contributions: Conceptualization, C.L. and R.T.; methodology, C.L. and R.T.; validation, C.L. and R.T.; formal analysis, C.L. and R.T.; investigation, C.L. and R.T.; resources, C.L. and R.T.; data curation, C.L. and R.T.; writing—original draft preparation, R.T.; writing—review and editing, C.L. and R.T.; visualization, C.L. and R.T.; supervision, C.L.; project administration, C.L.; funding acquisition, C.L. All authors have read and agreed to the published version of the manuscript.

Funding: This research is currently self-funded.

Informed Consent Statement: The consent to submit this paper has been received explicitly from all co-authors.

Data Availability Statement: The original contributions presented in this study are included in the article. Further inquiries can be directed to the corresponding authors.

Acknowledgments: This independent research effort was supported solely by the personal resources of the authors.

Conflicts of Interest: The authors declare no conflicts of interest.

References

1. Cai, W.; Daehn, G.; Vivek, A.; Li, J.; Khan, H.; Mishra, R.S.; Komarasamy, M.A. A state-of-the-art review on solid-state metal joining. *J. Manuf. Sci. Eng. Trans. ASME* **2019**, *141*, 031012. [CrossRef]
2. Wang, G.L.; Li, J.L.; Xiong, J.T.; Wang, W.L.; Ma, P.Y.; Zhang, F.S. Study on the friction interface evolution during rotary friction welding of tube. *J. Adhes. Sci. Technol.* **2019**, *33*, 1033–1046. [CrossRef]
3. Donohue, J.J. The friction welding advantage. *Weld. J.* **2001**, *80*, 30–34.

4. Li, W.; Liou, F.; Newkirk, J.; Taminger, K.M.B.; Seufzer, W.J. Investigation on Ti6Al4V-V Cr-Fe-SS316 multi-layers metallic structure fabricated by laser 3D printing. *Sci. Rep.* **2017**, *7*, 7977. [CrossRef] [PubMed]
5. Prasanthi, T.N.; Sudha, C.; Ravikirana; Saroja, S.; Kumar, N.N.; JanakiRam, G.D. Friction welding of mild steel and titanium: Optimization of process parameters and evolution of interface microstructure. *Mater. Des.* **2015**, *88*, 58–68. [CrossRef]
6. Kimura, M.; Iijima, T.; Kusaka, M.; Kaizu, K.; Fuji, A. Joining phenomena and tensile strength of friction welded joint between pure titanium and low carbon steel. *Mater. Des.* **2014**, *55*, 152–164. [CrossRef]
7. Dey, H.C.; Ashfaq, M.; Bhaduri, A.K.; Rao, K.P. Joining of titanium to 304L stainless steel by friction welding. *J. Mater. Process. Technol.* **2009**, *209*, 5862–5870. [CrossRef]
8. Lee, M.K.; Park, J.J.; Lee, J.G.; Rhee, C.K. Phase-dependent corrosion of titanium-tostainless steel joints brazed by Ag–Cu eutectic alloy filler and Ag interlayer. *J. Nucl. Mater.* **2013**, *439*, 168–173. [CrossRef]
9. Li, P.; Dong, H.G.; Xia, Y.Q.; Hao, X.H.; Wang, S.; Pan, L.W.; Zhou, J. Inhomogeneous interface structure and mechanical properties of rotary friction welded TC4 titanium alloy/316L stainless steel joints. *J. Manuf. Process.* **2018**, *33*, 54–63. [CrossRef]
10. Kim, Y.C.; Fuji, A.; North, T.H. Characterization and production mechanism of residual stress and plastic strain in titanium/AISI 304L stainless steel friction welds. *Q. J. Jpn. Weld. Soc.* **1994**, *12*, 243–248. [CrossRef]
11. Kale, G.B.; Patil, R.V.; Gawade, P.S. Interdiffusion studies in titanium–304 stain less steel system. *J. Nucl. Mater.* **1998**, *257*, 44–50. [CrossRef]
12. Mudali, U.K.; Ananda Rao, B.M.; Shanmugam, K.; Natarajan, R.; Raj, B. Corrosion and microstructural aspects of dissimilar joints of titanium and type 304L stainless steel. *J. Nucl. Mater.* **2003**, *321*, 40–48. [CrossRef]
13. Kim, S.Y.; Lee, W.B.; Koo, J.M.; Kim, D.U.; Yeon, Y.M.; Shur, C.C.; Jung, S.B. The joints characteristics of friction Welded titanium and 321 stainless steel. In *Titanium 2003 Science and Technology*; Wiley-VCH7; Wiley: Hoboken, NJ, USA, 2004; Volume 2, pp. 93–798.
14. Akbarimousavi, S.A.A.; GohariKia, M. Investigations on the mechanical properties and microstructure of dissimilar cp-titanium and AISI 316L austenitic stainless steel continuous friction welds. *Mater. Des.* **2011**, *32*, 3066–3075. [CrossRef]
15. Kimura, M.; Fuji, A. Characteristics of pure-titanium and low carbon steel friction welded joint with post-weld heat-treatment. *Mater. Sci. Technol.* **2016**, *32*, 1016–1024. [CrossRef]
16. Dong, H.; Yu, L.; Deng, D.; Zhou, W.; Dong, C. Effect of post-weld heat treatment on properties of friction welded joint between TC4 titanium alloy and 40Cr steel rods. *J. Mater. Sci. Technol.* **2015**, *31*, 962–968. [CrossRef]
17. Li, P.; Li, J.; Salman, M.; Liang, L.; Xiong, J.; Zhang, F. Effect of friction time on mechanical and metallurgical properties of continuous drive friction welded Ti6Al4V/SUS321 joints. *Mater. Des.* **2014**, *56*, 649–656. [CrossRef]
18. Li, X.; Li, J.; Liao, Z.; Jin, F.; Zhang, F.; Xiong, J. Microstructure evolution and mechanical properties of rotary friction welded TC4/SUS321 joints at various rotation speeds. *Mater. Des.* **2016**, *99*, 26–36. [CrossRef]
19. Liu, C.C.; Ou, C.L.; Shiue, R.K. The microstructural observation and wettability study of brazing Ti-6Al-4V and 304 stainless steel using three braze alloys. *J. Mater. Sci.* **2002**, *37*, 2225–2235. [CrossRef]
20. Kundu, S.; Ghosh, M.; Laik, A.; Bhanumurthy, K.; Kale, G.B.; Chatterjee, S. Diffusion bonding of commercially pure titanium to 304 stainless steel using copper interlayer. *Mater. Sci. Eng. A* **2005**, *407*, 154–160. [CrossRef]
21. Elrefaey, A.; Tillmann, W. Interface Characteristics and Mechanical Properties of the Vacuum-Brazed Joint of Titanium-Steel Having a Silver-Based Brazing Alloy. *Metall. Mater. Trans. A* **2007**, *38*, 2956–2962. [CrossRef]
22. Deng, Y.Q.; Sheng, G.G.; Xu, C. Evaluation of the microstructure and mechanical properties of diffusion bonded joints of titanium to stainless steel with a pure silver interlayer. *Mater. Des.* **2013**, *46*, 84–87. [CrossRef]
23. He, P.; Zhang, J.; Zhou, R.; Li, X. Diffusion bonding technology of a titanium alloy to a stainless steel web with an Ni interlayer. *Mater. Charact.* **1999**, *43*, 287–292. [CrossRef]
24. Shiue, R.K.; Wu, S.K.; Chan, C.H.; Huang, C.S. Infrared brazing of Ti-6Al-4V and 17-4 PH stainless steel with a nickel barrier layer. *Metall. Mater. Trans. A* **2006**, *37*, 2207–2217. [CrossRef]
25. Kundu, S.; Chatterjee, S. Interfacial microstructure and mechanical properties of diffusion-bonded titanium–stainless steel joints using a nickel interlayer. *Mater. Sci. Eng. A* **2006**, *425*, 107–113. [CrossRef]
26. Kurt, B.; Orhan, N.; Evin, E.; Çalik, A. Diffusion bonding between Ti–6Al–4V alloy and ferritic stainless steel. *Mater. Lett.* **2007**, *61*, 1747–1750. [CrossRef]
27. Lee, M.K.; Lee, J.G.; Choi, Y.H.; Kim, D.W.; Rhee, C.K.; Lee, Y.B.; Hong, S.J. Interlayer engineering for dissimilar bonding of titanium to stainless steel. *Mater. Lett.* **2010**, *64*, 1105–1108. [CrossRef]
28. Reddy, G.M.; Ramana, P.V. Role of nickel as an interlayer in dissimilar metal friction welding of Maraging steel to low alloy steel. *J. Mater. Process. Technol.* **2012**, *212*, 66–77. [CrossRef]
29. Muralimohan, C.H.; Ashfaq, M.; Ashiri, R.; Muthupandi, V.; Sivaprasad, K. Analysis and Characterization of the Role of Ni Interlayer in the Friction Welding of Titanium and 304 Austenitic Stainless Steel. *Metall. Mater. Trans. A* **2016**, *1*, 347–359. [CrossRef]

30. He, P.; Yue, X.; Zhang, J.H. Hot pressing diffusion bonding of a titanium alloy to a stainless steel with an aluminum alloy interlayer. *Mater. Sci. Eng. A* **2008**, *486*, 171–176. [CrossRef]
31. Kundu, S.; Sam, S.; Chatterjee, S. Interfacial reactions and strength properties in dissimilar titanium alloy/Ni alloy/microduplex stainless steel diffusion bonded joints. *Mater. Sci. Eng. A* **2013**, *560*, 288–295. [CrossRef]
32. Wang, L.X.; Liu, K.; Li, J.; Chen, Z.W.; Wang, J.; Okulov, A. Interfacial microstructure and mechanical properties of diffusion bonded joints of additive manufactured 17-4 PH stainless steel and TC4 titanium alloy. *Vacuum* **2024**, *219*, 112709. [CrossRef]
33. Zhang, M.; Cai, H.; Zhang, J.; Li, Q.; Wang, Y.; Huang, T.; Liu, J.; Wang, X. Interfacial bonding of CuZr metallic glass via oxide: A molecular dynamics study. *Corros. Sci.* **2021**, *182*, 109275. [CrossRef]
34. Ghorbal, G.B.; Tricoteaux, A.; Thuault, A.; Louis, G.; Chicot, D. Comparison of conventional Knoop and Vickers hardness of ceramic materials. *J. Eur. Ceram. Soc.* **2017**, *37*, 2531–2535. [CrossRef]
35. Ahmed, I.I.; Mohammed, A.T.; Abdulkareem, S.; Yahaya, T.; Ambali, I.O.; Bayode, B.L.; Adebisi, J.A. Potential of Cow Horn for Carbonitriding Treatment of Steel. *Waste. Biomass. Valori.* **2019**, *10*, 1969–1978. [CrossRef]
36. Pavan, P.; Talari, M.K.; Babu, N.K.; Rehman, A.U.; Srirangam, P. Effect of Heat Treatment on the Microstructure and Mechanical Properties of Rotary Friction Welded Dissimilar IN718 to SS304L Alloys. *Appl. Sci.* **2023**, *13*, 3584. [CrossRef]
37. Ajay, V.; Kumar, M.N.; Babu, N.K.; Kumar, T.M.; Krishna, K.V.; Reddy, G.M. Rotary friction welding of Inconel 718–AISI 304 stainless steel dissimilar joint. *Mater. Sci. Technol.* **2023**, *39*, 1950–1960. [CrossRef]
38. Gavalec, M.; Barenyi, I.; Krbata, M.; Kohutiar, M.; Balos, S.; Pecanac, M. The Effect of Rotary Friction Welding Conditions on the Microstructure and Mechanical Properties of Ti6Al4V Titanium Alloy Welds. *Materials* **2023**, *16*, 6492. [CrossRef] [PubMed]
39. Semiatin, S.L. An overview of the thermomechanical processing of α/β titanium alloys: Current status and future research opportunities. *Metall. Mater. Trans. A* **2020**, *51*, 2593–2625. [CrossRef]
40. Saju, T.; Velu, M. Fracture toughness and fatigue crack growth rate studies on rotary friction weldments of nickel-based superalloys. *Mater. Lett.* **2022**, *327*, 133027. [CrossRef]
41. van der Merwe, H.B.; James, M.N.; Hattingh, D.G.; Rall, W. Fatigue life prediction for rotary friction welded Ti-6Al-4V under variable amplitude fatigue loading. *Theor. Appl. Fract. Mech.* **2019**, *104*, 102321. [CrossRef]

Disclaimer/Publisher's Note: The statements, opinions and data contained in all publications are solely those of the individual author(s) and contributor(s) and not of MDPI and/or the editor(s). MDPI and/or the editor(s) disclaim responsibility for any injury to people or property resulting from any ideas, methods, instructions or products referred to in the content.